Bioelectrochemistry 158 (2024) 108711

Contents lists available at ScienceDirect

Bioelectrochemistry

journal homepage: www.journals.elsevier.com/bioelectrochemistry

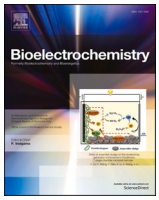

Anaerobic treatment of groundwater co-contaminated by toluene and copper in a single chamber bioelectrochemical system

Marco Resitano [a,1], Matteo Tucci [a,1], Alessio Mezzi [b], Saulius Kaciulis [b], Bruna Matturro [a,c], Emilio D'Ugo [d], Lucia Bertuccini [e], Stefano Fazi [a], Simona Rossetti [a], Federico Aulenta [a,c], Carolina Cruz Viggi [a,*]

[a] Water Research Institute (IRSA), National Research Council (CNR), 00010 Montelibretti, (RM), Italy
[b] Institute for the Study of Nanostructured Materials, National Research Council (CNR), 00010 Montelibretti, (RM), Italy
[c] National Biodiversity Future Center, Palermo 90133, Italy
[d] Department of Infectious Diseases, Istituto Superiore di Sanità, Rome, Italy
[e] Core Facilities, Istituto Superiore di Sanità, Rome, Italy

ARTICLE INFO

Keywords:
Electrobioremediation
Groundwater remediation
Microbial electrochemical technologies
Toluene
Copper

ABSTRACT

Addressing the simultaneous removal of multiple coexisting groundwater contaminants poses a significant challenge, primarily because of their different physicochemical properties. Indeed, different chemical compounds may necessitate establishing distinct, and sometimes conflicting, (bio)degradation and/or removal pathways. In this work, we investigated the concomitant anaerobic treatment of toluene and copper in a single-chamber bioelectrochemical cell with a potential difference of 1 V applied between the anode and the cathode. As a result, the electric current generated by the bioelectrocatalytic oxidation of toluene at the anode caused the abiotic reduction and precipitation of copper at the cathode, until the complete removal of both contaminants was achieved. Open circuit potential (OCP) experiments confirmed that the removal of copper and toluene was primarily associated with polarization. Analogously, abiotic experiments, at an applied potential of 1 V, confirmed that neither toluene was oxidized nor copper was reduced in the absence of microbial activity. At the end of each experiment, both electrodes were characterized by means of a comprehensive suite of chemical and microbiological analyses, evidencing a highly selected microbial community competent in the biodegradation of toluene in the anodic biofilm, and a uniform electrodeposition of spherical Cu_2O nanoparticles over the cathode surface.

1. Introduction

Petroleum hydrocarbons (PHs) and heavy metals (HMs) are the most frequent pollutants among all contaminated sites across Europe, as reported by Pérez and Rodríguez in a recent survey [1]. Both these classes of compounds have the potential to act as carcinogens, mutagens, or allergens in humans, and they can lead to a range of other toxic effects when they enter the aquatic food chain [2,3].

Most literature studies focused on the removal of a specific contaminant through a single mechanism, while achieving the simultaneous elimination of multiple pollutants continues to pose a challenge [4]. In fact, the different contaminants present in subsurface environments may possess different physicochemical properties, and the method implemented to remove one pollutant can inhibit the removal of other pollutants [5]. It is also important to underline that the co-occurrence of these compounds in contaminated sites is quite frequent, and their combined toxicity usually surpasses the sum of their individual toxic effect [6]. Combining multiple contaminant removal techniques into a single process can be advantageous in terms of versatility and economic benefits [7].

Numerous approaches have been investigated for the remediation of soil and water contaminated with a combination of PHs and HMs. Some approaches can be used to treat both soil and water contaminated by these pollutants, such as biological degradation [8,9] and extraction processes with surfactants and chelating solutions [10]. Other technologies are specific for water treatment, such as: adsorption on various

* Corresponding author.
E-mail address: carolina.cruzviggi@irsa.cnr.it (C. Cruz Viggi).
[1] These authors contributed equally to this work.

https://doi.org/10.1016/j.bioelechem.2024.108711
Received 20 December 2023; Received in revised form 10 April 2024; Accepted 12 April 2024
Available online 13 April 2024

carbon-based materials (e.g. activated carbon, magnetic ordered carbon, lignite, etc.) [11,12], photocatalytic reduction [13,14], and electrochemical methods, like capacitive deionization combined with electro-oxidation hybrid systems [15] and electrocoagulation with Fenton processes utilizing sacrificial anodes [16].

In recent years, bioelectrochemical systems (BESs) are attracting increasing attention as a promising alternative to conventional remediation strategies. BESs can provide a virtually endless reservoir of electrons, to support microbial metabolism through solid electrodes, that can potentially serve as virtually inhexustible electron donors (i.e., as cathodes) or electron acceptors (i.e., as anodes) for prompting reduction or oxidation of contaminants, respectively. Electrodes can thus avoids the disadvantages associated with the introduction of air, oxygen, or other chemicals into the aquifer [17], thereby making the treatment process greener and more sustainable. Microbial electrolysis cells (MECs) are a type of BESs in which an electric potential is applied to the electrodes to facilitate otherwise slow or energetically unfavourable oxidation reactions at the (bio)anode and/or reduction reactions at the (bio)cathode [18]. MECs have been applied for the treatment of PHs at the anode [19–26] or removal and recovery of HMs at the cathode [27–31]. However, there have been only limited attempts to address the simultaneous degradation in electrified systems of both PHs and HMs.

Few notable examples include the work of Chen et al. [15], where the combination of capacitive deionization and electro-oxidation (CDI-EO) achieved the simultaneous removal of heavy metals and organic contaminants within a single apparatus. Notably, it achieved the removal of Cu^{2+} ions through cathodic electrosorption and electrodeposition. Another noteworthy study employed electrochemical Fenton treatment for the concurrent removal of heavy metals and organic pollutants from surface finishing wastewater [16]. In another study, Zhang et al., developed a highly efficient treatment approach for real wastewater containing organic matter, heavy metals, and sulfate, employing a sulfur-cycle-mediated Microbial Fuel Cell (MFC) [32]. Lastly, Gambino et al. focused their work on the simultaneous removal of organic matter and heavy metals from marine sediment through the utilization of sediment-based microbial fuel cells (SMFCs) [33].

In the above cited papers, the investigated matrix typically consisted of wastewaters or sediments/soils, and the oxidizable component was represented by undefined “organic substances” present in the wastewaters, and not specifically by petroleum hydrocarbons.

To the best of our knowledge, no prior studies have explored the application of bioelectrochemical processes for the concurrent treatment of groundwater contaminated with PHs and HMs.

Our previous studies proved the efficacy of bioelectrochemical systems in simultaneously treating multiple groundwater contaminants, paving the way for the application in real-world scenario [20,25,34,35]. We demonstrated that oxidizable and reducible contaminants could be efficiently removed in a single stage bioelectrochemical treatment. The oxidizable compounds treated at the anode were represented by toluene as model substrate, while at the cathode sulphate [25], trichloroethene [34] and chloroform [35] have been degraded by reductive biological processes.

In this work, we studied for the first time the application of a bioelectrochemical system to the simultaneous removal PHs and HMs from contaminated groundwater with a membrane-less single-chamber reactor. The configuration of the reactor was different from that used in the previous studies, as well as the feeding and operational conditions. The system was spiked with toluene as model PH and Cu^{2+} as model HM. Toluene was chosen as model contaminant because it’s widely studied as model contaminant being one of the most pervasive soil and groundwater pollutant due to its high mobility and water solubility [36]. Copper was chosen being one of the most studied metals in BES studies for HM recovery from contaminated waters [27–31]. The removal of toluene at the anode, together with the reduction and precipitation of copper at the cathode were evaluated. Overall, this study provides evidence for a novel application of bioelectrochemical systems for the remediation of sites polluted with mixtures of toluene and copper, which can then be applied to sites contaminated by other combinations of pH and HM.

2. Experimental

2.1. Experimental setup and operations

The experimental setup used in this study consisted in single-chamber bioelectrochemical cells, from now on referred to as *E-cell*, made of gastight borosilicate glass bottles sealed with Teflon-faced butyl rubber stoppers, having a total volume of 250 mL. The cells had a two-electrode configuration and were equipped with two graphite rods (purity: 99.995 %, length: 7.5 cm, ø: 0.6 cm; Sigma-Aldrich), one serving as anode and the other as cathode, with a potential difference of 1 V applied between them by an IVIUMnSTAT potentiostat (IVIUM Technologies). The chosen cell voltage was high enough to address potential losses and support electrode reactions at the highest possible rates, yet below the value that would favour water electrolysis. The anode and the cathode coexisted in the single-chamber cell without physical separation. The nominal surface area of the electrodes (calculated by taking into account only the part of the electrode that was immersed in the liquid phase) was 9.7 cm^2. The distance between the anode and the cathode was approximately 2 cm. Titanium wires (ø: 0.81 mm, Alfa Aesar) connected the anode and the cathode to the potentiostat. Each cell was filled with 180 mL of anaerobic mineral medium [37], the composition of which is reported in the Supporting Information (Tab S1). Upon setup, the cells were flushed with a N_2/CO_2 (70:30 v/v) gas mixture to establish anaerobic conditions, and the pH was maintained at a value of about 7 by adding an anaerobic solution of bicarbonate (10 % w/v) as a buffer.

At the start of the experimentation, two replicated cells were inoculated with 20 mL of groundwater from a PH-contaminated site in Italy. The groundwater contained electroactive bacteria capable of degrading hydrocarbons, as confirmed by previous experiments [34,35]. In parallel, different control experiments (each in duplicate) were also set up. These included abiotic, non-polarized tests, carried out using an identical experimental setup as in the *E-cell*, with the aim of assessing the possible contribution of abiotic adsorption mechanisms on the observed toluene and copper removal. Similarly, abiotic and polarized tests were carried to evaluate the possible contribution of electrochemical reactions on toluene and copper removal. The cells were kept out at room temperature (25 ± 2 °C) and in the dark to avoid the growth of photosynthetic microorganisms. Throughout the study, the cells were spiked with toluene (5 mg/L) and Cu^{2+} (10 mg/L) at the start of successive cycles, as reported in Table 1. Copper was spiked in Run III-V, after evaluating that an electroactive biofilm had established on the anodes during Runs I and II. Regarding toluene and copper, added concentrations were those commonly found in contaminated groundwater.

The cells were regularly sampled and analysed for toluene, gases and copper concentration. Electrochemical potentiostatic measurements were carried out with the potentiostat.

Table 1
Main operating conditions applied during the different experimental runs.

Run	Operational period (days)	Polarization (V vs. SHE)	Toluene concentration (mg/L)	Cu^{2+} concentration (mg/L)
I	1–7	1.0	5	0
II	8–14	1.0	5	0
III	15–52	1.0	5	10
IV	53–101	1.0	5	10
V	102–122	– (Open circuit potential)	5	10

2.2. Analytical methods

Gaseous samples were taken from the cells using gastight syringes and analyzed for toluene and other gases using a gas-chromatograph (Agilent 8860, GC system) equipped with a flame ionization detector (FID) and a thermal conductivity detector (TCD). Gas-phase concentrations were converted into liquid-phase concentrations using tabulated Henry's Law constants [38]. The GC method, calibration ranges and LOD of analytical methods are reported in the Supporting Information (Tab S2).

Liquid samples were filtered (nylon filters, pore size 0.2 mm, 47 mm diameter, Nuclepore), immediately acidified with 1 % HNO_3 Suprapur (Sigma-Aldrich) and analyzed by ICP-OES (Model 5800, Agilent) to determine the bulk liquid Cu concentration.

2.3. Microscopy analysis of the microbial communities

In order to visualise the 3D structure of the biofilms grown on the graphite electrodes, cells were stained with 4′,6-diamidino-2-phenylindole (DAPI) solution, at room temperature in the dark for 15 min, followed by a second staining of 0.15 mM calcofluor-white (Sigma-Aldrich Chemie GmbH), at room temperature in the dark for 4 min, for EPS visualization. The stained biofilms were then observed under a confocal laser scanning microscope (CSLM; Olympus FV1000). Both cells and EPS of each biofilm were excited by 405 nm light and emitted at 430 to 470 nm (blue color). Graphite surface was visualized by its reflection signal (635 nm line of a diodo laser). The three-dimensional reconstruction of CSLM images was elaborated by the software IMARIS 7.6 (Bitplane) with 3D volume rendering mode.

2.4. DNA extraction and high-throughput 16S rRNA gene sequencing

The bulk effluent (20 mL) and the graphite rods (both anode and cathode) were collected at the end of the experiment. Graphite rods were vortexed in 40 mL PBS 1X (8 g/L of NaCl, 0.2 g/L of KCl, 1.44 g/L of Na_2HPO_4, 0.24 g/L of KH_2PO_4) for 15 mins in order to disrupt the biofilm grown on the rods surface. The effluent and the PBS-suspended biofilm were filtered through hydrophilic polycarbonate membranes (0.2 μm pore size, 25 mm diameter, Millipore) and immediately used for DNA extraction. DNA was extracted by using the DNeasy PowerLyzer PowerSoil Kit (QIAGEN) according to the manufacturer's instructions. 4 ng of DNA were used a template for library construction via PCR amplification targeting the V1–V3 region of the 16S rRNA gene (primers 27F: 5′-AGAGTTTGATCCTGGCTCAG-3′; 534R: 5′-ATTACCGCGGCTGCTGG-3′). The V1–V3 region of the 16S rRNA gene was specifically targeted due to its well-established utility in identifying bacterial taxa within microbial communities. PCR reactions were conducted in a total volume of 25 μL, comprising Phusion Master Mix High Fidelity (Thermo Fisher Scientific) and 0.5 μM of 27F and 534R primers with adaptors. All PCR reactions were performed in duplicate and subsequently pooled. The amplicon libraries were purified using Agencourt® AMpureXP-beads (Beckman Coulter), and their concentrations were measured using a Qubit 3.0 fluorometer (Thermo Fisher Scientific). The purified libraries were equimolarly pooled and then diluted to 4 nM. A Phix control was added at a 10 % ratio to the pooled libraries. Subsequently, the samples were paired-end sequenced (2 × 301 bp) on a MiSeq instrument (Illumina) using a MiSeq Reagent kit v3, 600 cycles (Illumina), following standard guidelines. The procedure employed for library preparation has been also reported elsewhere [35,39,40]. Bioinformatic analysis was performed after checking read quality with FastQC software (v 0.11.7), as reported elsewhere [41]. The Silva 132–99 database was used to assign the taxonomy (release December 2017, https://www.arb-silva.de/documentation/release-132/). A dataset of amplicon sequence variants (ASVs) was generated including 3767 ASVs from the cathode, 17,410 ASVs from the anode and 32,231 ASVs from the bulk effluent. Sequencing data have been deposited in the DDBJ/ENA/GenBank under the BioProject PRJNA1039752.

2.5. X-ray photoelectron spectroscopy of graphite electrodes

The surface chemical composition of the graphite rods was assessed through X-ray photoelectron spectroscopy (XPS). This analysis was conducted using a VG Escalab MkII spectrometer (VG Scientific Ltd) equipped with a 5-channeltron detection system and an unmonochromatized radiation source of Al Kα (1486.6 eV). Spectra were registered in selected-area mode, operating with electrostatic lenses and fixing the entrance slit of analyser at A3x12, to collect photoelectrons from a sample area of about 3 mm diameter. The binding energy (BE) scale was calibrated positioning the C1s peak of graphite at BE = 284.6 eV. All the spectra were acquired at the pass energy of 50 eV. Spectroscopic data were acquired and processed using Avantage v.5 software, using a peak-fitting routine with Shirley background and Scofield sensitivity factors for elemental quantification.

2.6. Scanning electron microscopy (SEM) and energy Dispersive spectroscopy (EDS) of graphite electrodes

The graphite electrodes were broken into small pieces, fixed with glutaraldehyde 2.5 % in Na-cacodylate buffer 0.1 M for 1 h at room temperature, washed in buffer and post-fixed with osmium tetroxide 1 % in 0.1 M Na-cacodilate for an additional 1 h. After rinsing, samples were dehydrated through a graded series of ethanol solutions, from 30 % to 100 %. Then, ethanol was gradually substituted by hexamethyldisilazane (HMDS) through an incubation of 30 min in 1:1 (ethanol: HMDS) solution, followed by pure HMDS for 1 h and then by a final drying process under chemical hood for 1 h (totally removing HMDS and leaving to evaporate all the liquid phase). The dried graphite rods were mounted on aluminium stubs with silver paint, carbon coated and analyzed by FE-SEM Quanta Inspect F (FEI – Thermo Fisher Scientific) equipped with an EDAX detector used for the EDS analysis on the cathode surface.

2.7. Calculations

The coulombic efficiency (CE) for each cycle was calculated as the ratio between the transferred charge (that is the integral of the electric current over time) and the theoretical charge deriving from the oxidation of the toluene, according to the following equation:

$$CE(\%) = \frac{\int i(t) \times dt}{\Delta_{tol} \times 36 \times F} \quad (1)$$

where i is the measured electric current (mA), F is the Faraday's constant, Δ_{tol} is the amount of removed toluene (mmol) and 36 is the number of mmol of electrons released from the complete oxidation of 1 mmol of toluene.

The cathode capture efficiency (CCE) of each cycle was calculated as the ratio between the cumulative equivalents of produced methane ($mmoleq_{CH4}$) and the cumulative equivalents deriving from current ($mmoleq_i$), according to the following equation:

$$CCE(\%) = \frac{mmoleq_{CH4}}{mmoleq_i} \quad (2)$$

3. Results and discussion

3.1. Bioelectrochemical experiments

From the chemical analysis, it can be observed that toluene was removed almost completely (95 % and 99 % of removal in Run I and II, respectively), and the duration of the cycles was relatively short (around 6 days for each cycle), pointing to the presence at the anode of an electroactive biofilm capable of efficiently oxidizing toluene. As shown

in Fig. 1A, the rapid and quantitative toluene depletion during the first two cycles corresponded to two current peaks of 0.06 and 0.04 mA, respectively. When toluene was completely depleted, the current dropped to the initial values in both cycles. This fact indicates that current generation was dependent on the presence of toluene, which most likely served as the main carbon and energy source for the anodic biofilm.

The resulting average CEs were 62.9 ± 7.9 % and 72.1 ± 16.7 % in the first and in the second run, respectively. It can be hypothesized that toluene was converted into electric current through the formation of intermediates, such as VFA (Volatile Fatty Acids), which accumulated in the cells medium and were not totally converted into current, as indicated by CEs substantially lower than 100 %. In a previous work, it was found that the bioelectrochemical degradation of toluene proceeded via a syntrophic pathway involving cooperation between different microbial populations. Firstly, hydrocarbon degraders quickly converted toluene into metabolic intermediates probably by breaking the aromatic ring upon fumarate addition. Subsequently, fermentative bacteria converted these intermediates into volatile fatty acids (VFA) and likely H_2, which were then used as substrates by electroactive microorganisms forming the anodic biofilm [19]. A similar removal mechanism can therefore be hypothesized. Methane production started immediately at the beginning of both cycles, reaching concentrations of 0.25 and 0.21 mg/L in Run I and II, respectively (Fig. 1C).

Average values of CCEs of 72.9 ± 6.6 % and 86.3 ± 9.4 % were calculated in Run I and II, respectively. These fairly high CCE values are consistent with methane production being driven by the hydrogen produced at the cathode (Fig. 5).

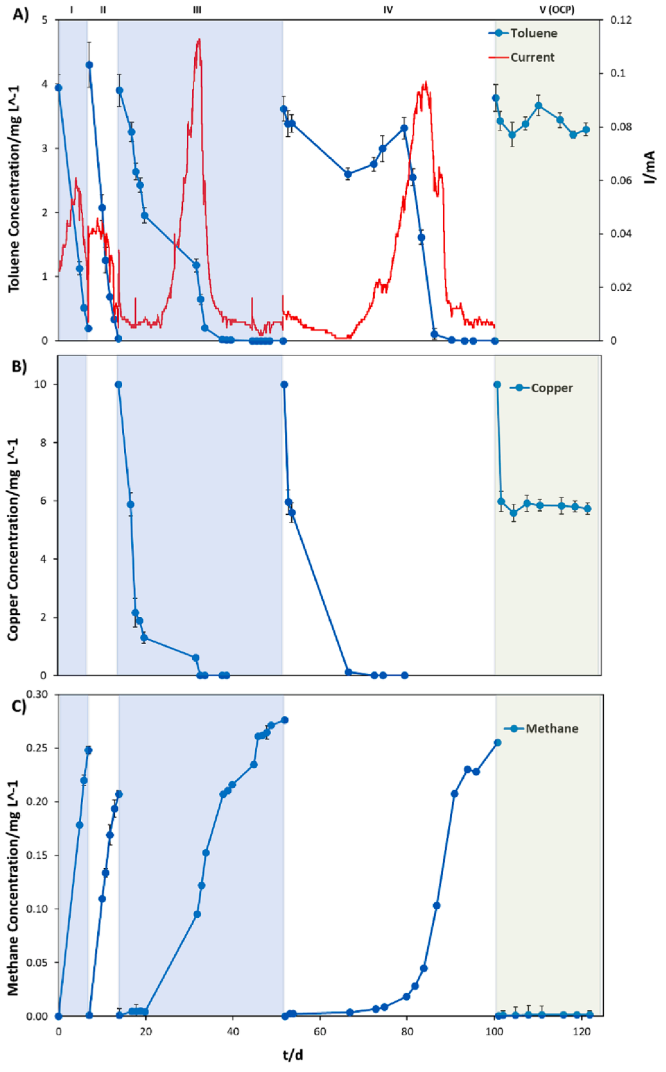

Fig. 1. Performances of the bioelectric cell. Trends of: A) toluene removal and current generation; B) copper removal; C) methane production.

Since after Runs I and II an electroactive biofilm was well established on the anodes, toluene was added along with copper (in the form of Cu^{2+}) to assess the possibility of simultaneously removing hydrocarbons and heavy metals through bioelectrochemical processes. In both cycle III and IV, the presence of Cu^{2+} significantly slowed down the removal of toluene, likely due to inhibition phenomena. Many bacterial species are efficiently killed on copper or copper alloy surfaces. It is thought that contact killing proceeds by a mechanism whereby the metal-bacterial contact damages the cell envelope, which, in turn, makes the cells susceptible to further damage by copper ions [42]. Nevertheless, toluene was completely removed in both cycles. Despite toluene removal was slower and substantially delayed (particularly during Run IV) compared to the cycles carried out in the absence of Cu^{2+}, current production reached remarkably higher current peaks accounting to 0.09–0.11 mA (Fig. 1A), thus nearly doubling the values recorded in the previous cycles (Run I and II). The corresponding CE were higher than 200 % in both cycles. This finding could be due to two different factors: the hydrogen formed at the cathode was partially re-oxidized at the anode via a so-call electron recycling process [43], and/or the intermediates of toluene (such as VFA, as above mentioned), that had been accumulated during the first two feeding cycles, were now fully and more rapidly oxidized at the anode, resulting in high current peaks. Further investigations would be warranted to shed light on this interesting behavior.

Regarding copper, its concentration decreased significantly immediately after addition in both cycles, likely because of adsorption phenomena onto the graphite electrodes. After this initial rapid removal mechanism, copper concentration progressively decreased down to values below instrumental detection limits in both cycles (Fig. 1B), thus confirming the possibility of simultaneously removing toluene and copper through bioelectrochemical oxidation and cathodic reduction, respectively.

Copper addition also slowed down methane production during cycle III and IV, although ultimately methane reached even higher concentrations than in the previous cycles, also in line with the higher generated electric current (Fig. 1C). On the contrary, the cathode capture efficiencies (towards methane production) decreased. In fact, CCEs of 38.7 ± 0.5 % and 35.3 ± 10.3 % were calculated in Run III and IV, respectively. The cathode capture efficiencies decreased since in these cycles the hydrogen was no longer only converted into methane, but it was also re-oxidized at the anode, as previously hypothesized. Copper electro-reduction may also have contributed (up to 20 %, based on the removed copper) to reducing the yield of conversion of electric current into methane.

During the last operational run (V), the circuits of the two bioelectrochemical cells were disconnected and maintained at open circuit potential (OCP) after toluene and copper were added. Upon removal of polarization, toluene degradation ceased almost immediately, as well as the production of methane. Except for the sharp decrease observed right after its addition, which is likely due to adsorption phenomena, copper concentration remained constant throughout the OCP cycle. This evidence confirms that the removal in the previous cycles was primarily dependent by the polarization.

An additional experiment was conducted using two identical cells without inoculum and not connected to the potentiostat, to assess the possible adsorption of copper onto graphite rods or other abiotic mechanisms involved in the copper removal. Control cells were operated in batch mode for about 120 days, showing an initial decrease after metal addition likely due to adsorption phenomena, and remaining approximately constant throughout the experiment (Figure S1). The trend of copper concentration observed in these abiotic and non-polarized experiments was similar to the one observed in the OCP run.

Finally, an abiotic and polarized experiment was performed, to

evaluate the possible contribution of electrochemical reactions on copper removal. This last experiment evidenced the absence of significant copper and toluene removal in not inoculated conditions, even when a potential difference of 1 V is applied between the anode and the cathode (Figure S2).

To summarize, the following removal mechanism can be hypothesized: during polarization toluene was converted into metabolic intermediates (such as VFAs), which were in turn oxidized at the anode, generating an electric current that was used at the cathode for the reduction and precipitation of copper (Fig. 2). Further insights into the mechanisms of contaminants removal are gathered through electrodes characterization.

3.2. Electrodes characterization

At the end of the experiment, graphite rods were collected for the microbiological characterization of the biofilm and the analysis of the chemical composition of the surface. Electrodes characterization was aimed at clarifying the mechanisms of contaminants removal observed in the bioelectrochemical experiments.

3.2.1. Anode characterization

The anode collected from the cells at the end of the experimental period was divided in different parts for subsequent microbiological, microscopy and spectroscopy analyses.

Fig. 2A shows the CLSM combined images showing the spatial distribution (X − Y, X − Z, and Y − Z planes) of DAPI stained cells and EPS (stained by Calcofluor White) attached to the graphite electrode used as anode. The CLSM revealed the presence of a nearly 20 μm-thick biofilm on the surface of the electrode. Both cells and EPS are blue, while the surface of the electrode is visualized by its reflection signal in the same microscopic field, and appears grey. The presence of a biofilm was confirmed by SEM images of the anode (Fig. 2B), which show an electrode uniformly covered by a biofilm, mostly composed by bacilli (morphology: ~1 μm long and 0.5 μm wide) and to a lesser extent by cocci.

The 16S rRNA gene amplicon sequencing revealed a highly selected microbial community of the biofilm collected at the end of the experiment from the anode surface and the bulk effluent (Fig. 3). The bacterial composition of the bulk effluent was also analyzed. In particular, the anodic biofilm was dominated by members of the class of *Alphaproteobacteria* (41 %) and members of *Actinobacteria* (40 %) and *Firmicutes* (11 %) phyla. They were all previously identified in bioelectrochemical systems and reported to be involved in the syntrophic degradation of aromatic hydrocarbons, as detailed below.

The most abundant bacterial taxa found on the anode surface were *Rhizobiaceae* (39.5 % of total reads). Similarly, also within the bulk effluent, *Rhizobiaceae* were dominant (68 %). Members of this family have been reported to be involved in the degradation of aromatic hydrocarbons [44–46]. In particular, the single sequence ASV1 (Tab S3) was the most abundant found on the anode surface and in the bulk effluent of the bioelectrochemical reactor developed in the current study. The ASV1 sequence shows 100 % similarity (BLAST analysis, RID: NENPHDUZ013) with *Aminobacter* species, the latter previously identified as genera capable of degrading toluene in polluted environments [47], and also found in anode microbial communities in MFCs [48]. Interestingly, *Rhizobiaceae* were highly abundant also in the bioelectrochemical reactor of a previous study treating toluene, where the authors hypothesized that it could drive the degradation of toluene leading to the production of key intermediates useful for the subsequent fermentative processes for VFA and H_2 production [19]. Other taxa present in the biofilm on the anode surface were affiliated with *Actinobateria*, including *Coriobacteriia_OPB41* (30 %) and *Cellulomonadaceae_Actinotalea* (7 %). A direct involvement of unidentified members of Actinobacteria order OPB41 in toluene or hydrocarbons degradation was not discussed so far even though they were reported as a component of microbial community in previous works concerning hydrocarbons degradation [19,35,49,50]. Anyway, Khomyakova and colleagues have recently isolated two pure cultures of anaerobic actinobacteria belonging to *OPB41* [51]. In particular, strain M08DHBT has the ability to grow on the aromatic compound 3,4-dihydroxybenzoic acid. This compound, with a trivial name protocatechuate, could be formed during aerobic or anaerobic degradation of lignin-associated phenolic compounds. Analysis of strain M08DHBT genome did not reveal any complete aerobic or anaerobic pathways of aromatic compounds degradation, but some crucial determinants of protocatechuate oxidation have been identified.

Actinotalea was recently identified in the anodic community of a MFC [52]. Szydlowski and colleagues identified the presence of numerous sequences related to electron transfer in its genome, e.g., the type IV

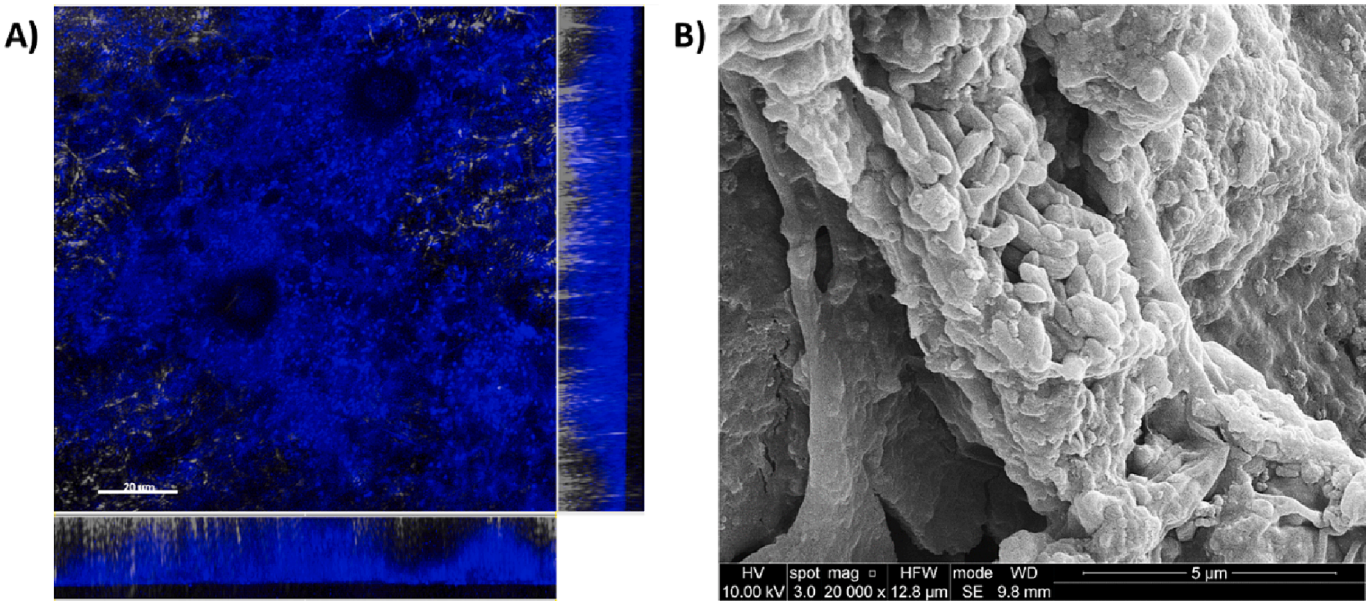

Fig. 2. A) CLSM combined images showing the spatial distribution (X − Y, X − Z, and Y − Z planes) of DAPI stained cells and EPS attached to the graphite electrode used as anode. B) SEM micrograph of the anodic biofilm. Both CLSM and SEM images were taken at the end of the cells operation.

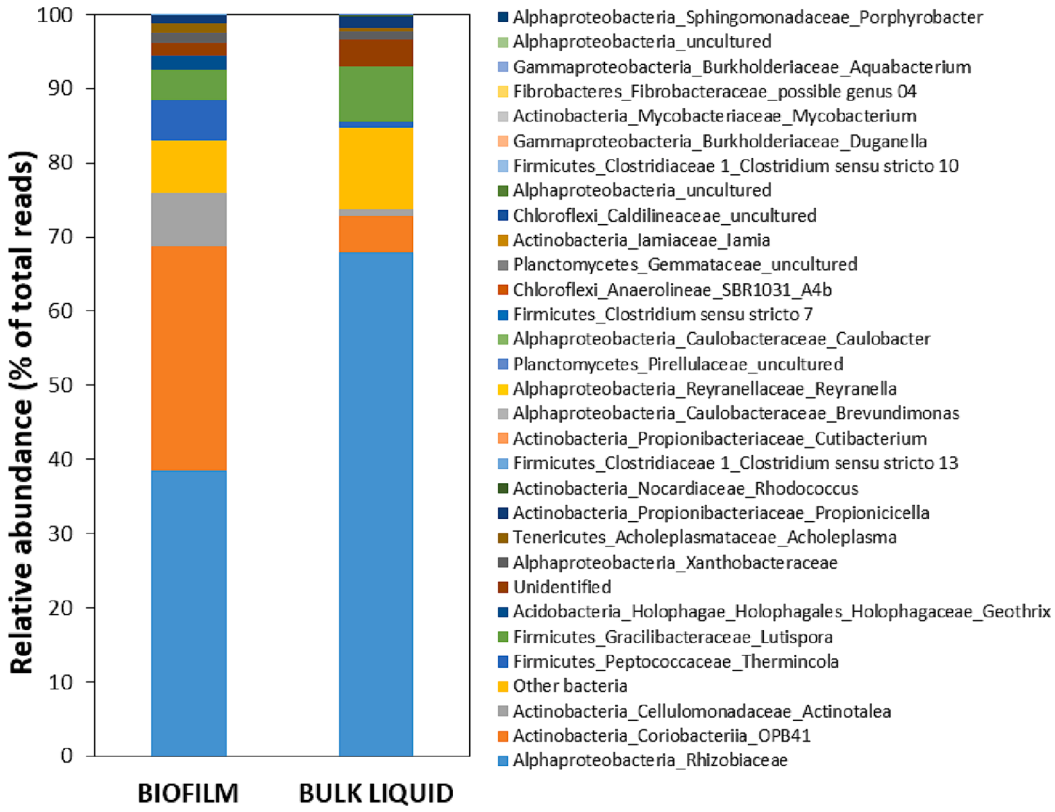

Fig. 3. Bacterial community composition revealed by the 16S rRNA gene amplicon sequencing. Data are reported as the relative abundance of ASVs as a percentage of total reads in both the biofilm on the anode surface and the bulk liquid.

pilus biosynthesis gene pilB, confirming that this organism can respire through anodes, just like the model electrogenic microorganism *Geobacter*. They also documented the presence of novel and unique enzymes, such as NADH translocases, that could provide resilience to high Cu content. *Actinotalea* is also reported to be involved in aromatic hydrocarbons degradation [53,54] both in electrified [54] and in not electrified [53] systems. Both kind of the cited systems were amended with electrically conductive particles of biochar.

Member of *Firmicutes,* such as *Peptococcaceae_Thermincola* (5.5 %) and *Gracilibacteraceae_Lutispora* (5 %), were also found on the anode surface. *Firmicutes* were also found to be involved in the anaerobic biodegradation of polycyclic aromatic hydrocarbons (PAHs). Members of this family were the most abundant microorganisms in bioaugmented inocula for the remediation of PAH contaminated soils [55]. *Firmicutes* were also identified in the bioanode biofilm of BES for accelerating the anaerobic biodegradation of Resorcinol, a typical aromatic contaminant as well as a key central intermediate (other than benzoyl-CoA) involved in anaerobic biodegradation of aromatics [56].

In particular, *Thermincola* members have been previously found in a toluene/TCE degrading bioelectrochemical reactor [34], as well as in a tubular microbial fuel cell to remove benzene and toluene, together with the exoelectrogens *Geobacter* as the main species on the anodic surface [57]. These previous evidences suggest a role of T*hermincola* member in toluene biodegradation. Regarding the *Lutispora* member found on the anode surface, it has been previously reported this microorganism as key degrader of VFA, which end products are acetate, isobutyrate, propionate and isovalerate [58], thus suggesting a role in the VFA metabolism within the system.

As expected, the bulk effluent showed a similar composition to the anode biofilm, with *Alphaproteobacteria* (70 %), *Actinobacteria* (11 %) and *Firmicutes* (9.8 %).

Overall, the microbiological characterization of the electrogenic biofilm revealed a highly selected bacterial community competent in the biodegradation of toluene. It is likely that members of Rhizobiaceae, particularly Aminobacter, along with Coriobacteriia_OPB41, and to a lesser extent Peptococcaceae_Thermincola, are the primary bacterial players responsible for toluene degradation within the system, while Lutispora likely contributes to toluene transformation into VFAs.

X-ray photoelectron spectroscopy was finally employed to identify the chemical species present on the surface of the graphite rods retrieved at the end of the experiment. For comparative purposes, an identical, unused graphite rod was also analyzed. Besides trace amounts of impurities mainly consisting of silicon (as SiO_2), oxygen (as OH^-), and alumina (as Al_2O_3), photoemission spectra of the untreated graphite rod revealed only the presence of graphitic carbon (C 1 s spectrum, C–C bond at 284.6 eV).

In contrast, the C 1 s spectrum of the anode clearly revealed, in addition to graphite, a second component at 288.2 eV due to the bonds of C = O and/or C-N, most likely attributable to the presence of adherent bacterial cells. Consistently, the nitrogen spectrum revealed the presence of N 1 s peak located at BE = 400.4 eV, which is characteristic for C = NH, C-NH_2 bonds.

3.2.2. *Cathode characterization*

The cathode collected at the end of the experiment was partitioned into various segments for subsequent analysis. The surface of the cathodes coming from the electrified cells showed a reddish coloration to the naked eye, which is typical of copper deposition.

The microbiological characterization of the cathode revealed a very low number of ASVs (3767) from the 16S rRNA gene sequencing with a heterogeneous bacterial composition, confirming that no significant biological process took place at the cathode.

As proof of this, SEM images of the cathode (Fig. 4) showed no significant presence of microorganisms and confirmed uniform Cu electrodeposition over the surface of the cathode. Specifically, it can be observed the presence of spherical copper nanoparticles, with size

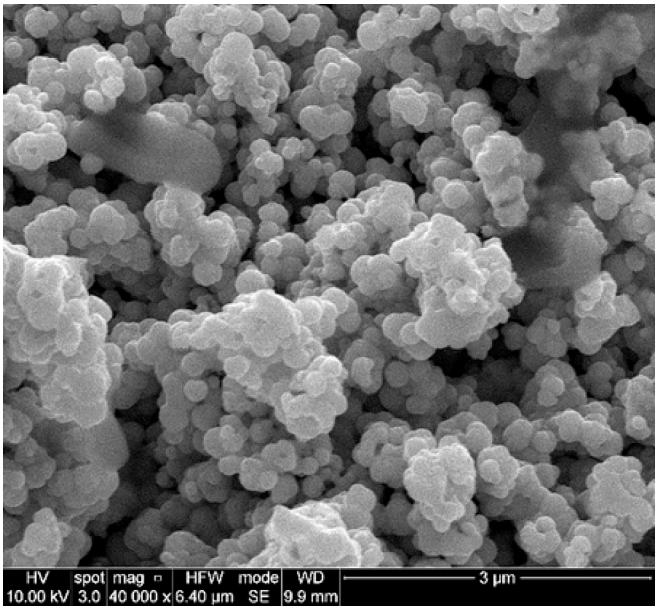

Fig. 4. SEM micrograph of the spherical copper nanoparticles at the cathode surface. SEM images were taken at the end of the cells operation.

ranging between 200 and 300 nm.

Copper nanostructures have recently garnered significant attention in the literature. This is primarily because the face-centered cubic structure of copper is considered an ideal alternative material, owing to its remarkable stability, excellent electrical conductivity, catalytic properties, and cost-effectiveness when compared to metals such as silver and gold [59,60]. Various shapes of copper nanostructures, including cubes, prisms, spheres and wires, have been obtained using a variety of techniques of deposition [61]. Electrochemical deposition stands out as a promising method for making copper nanoparticles due to its user-friendliness and cost-effectiveness. Several research groups have reported the synthesis of spherical copper nanoparticles similar to those obtained in this study through electrodeposition techniques [61–64].

Energy Dispersive Spectroscopy (EDS) analysis was performed in five different spots, as showed in Figure S3, to determine the elemental composition of the cathodic deposit. The EDS measures resulted in an average atomic ratio of Cu:O = 2.07 ± 0.14 % (Figure S4), confirming that copper was abiotically reduced and deposited at the cathode as Cu_2O.

Copper electrodeposition as cuprous oxide was confirmed by XPS analysis, which revealed, in addition to what was found for the anode (peaks related to graphite, bonds of C = O and/or C-N and bonds of C = NH, C-NH_2, all attributable to bacterial cells, although the latter are present in smaller percentages), the presence of Cu peaks at 933.2 eV attributable to Cu_2O and Cu peaks at 935.5 eV most likely assigned to Cu $(OH)_2$.

4. Conclusions

For the first time, the degradation of toluene was coupled with copper removal in a single-chamber bioelectrochemical cell. The system was able to achieve almost complete removal of both toluene and copper, exploiting both the oxidation and the reduction reaction simultaneously. Through a comprehensive set of chemical and microbiological analyses, the mechanism of contaminants removal was elucidated: toluene was oxidized at the bioanode, generating an electric current that was used at the cathode for the abiotic reduction and precipitation of copper. Electrodes characterization evidenced a highly selected and competent microbial community in the anodic biofilm, directly engaged in the biodegradation of toluene, and a uniform electrodeposition of spherical copper nanoparticles across cathode surface.

The herein studied bioelectrochemical process is at an initial stage of development and would warrant further investigations in order to single out the operating conditions for contaminants removal, primarily in terms of reactor design, electrode materials, and applied working conditions (e.g., cell voltage). It would also be interesting to assess process performance in the presence of even more complex mixtures of contaminants to verify the possible occurrence of competitive effects. The recovery of metal nanoparticles from the electrode can possibly open new opportunities in the broad area of the valorization of contaminated (waste)water from a circular economy perspective.

CRediT authorship contribution statement

Marco Resitano: Writing – original draft, Visualization, Investigation, Formal analysis, Conceptualization. **Matteo Tucci:** Writing – original draft, Visualization, Investigation, Formal analysis, Conceptualization. **Alessio Mezzi:** Writing – review & editing, Investigation, Formal analysis. **Saulius Kaciulis:** Writing – review & editing, Formal analysis. **Bruna Matturro:** Writing – review & editing, Investigation, Formal analysis. **Emilio D'Ugo:** Writing – review & editing, Formal analysis. **Lucia Bertuccini:** Writing – review & editing, Investigation,

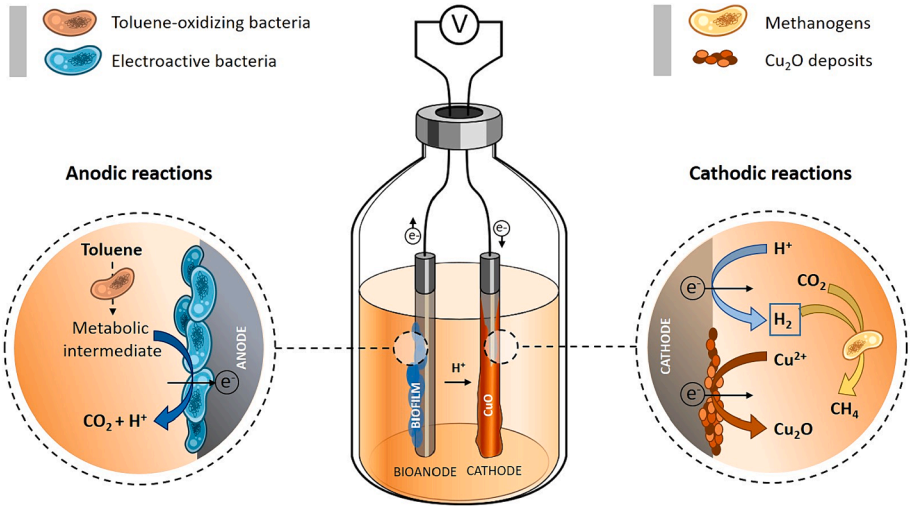

Fig. 5. Schematic proposed mechanisms for the bioelectrochemical treatment of a groundwater co-contaminated by toluene and copper.

Formal analysis. **Stefano Fazi:** Writing – review & editing, Formal analysis. **Simona Rossetti:** Writing – review & editing, Project administration, Funding acquisition, Conceptualization. **Federico Aulenta:** Writing – review & editing, Project administration, Funding acquisition, Conceptualization. **Carolina Cruz Viggi:** Writing – original draft, Visualization, Supervision, Methodology, Formal analysis, Conceptualization.

Declaration of competing interest

The authors declare that they have no known competing financial interests or personal relationships that could have appeared to influence the work reported in this paper.

Data availability

Data will be made available on request.

Appendix A. Supplementary material

Supplementary data to this article can be found online at https://doi.org/10.1016/j.bioelechem.2024.108711.

References

[1] A. Payá Pérez, N. Rodríguez Eugenio, Status of local soil contamination in Europe – Revision of the indicator "Progress in the management contaminated sites in Europe," Publications Office, 2018. Doi: 10.2760/093804.

[2] J. Tang, M. Wang, F. Wang, Q. Sun, Q. Zhou, Eco-toxicity of petroleum hydrocarbon contaminated soil, J. Environ. Sci. 23 (2011) 845–851, https://doi.org/10.1016/S1001-0742(10)60517-7.

[3] S.S. Sonone, S. Jadhav, M.S. Sankhla, R. Kumar, Water contamination by heavy metals and their toxic effect on aquaculture and human health through food chain, Lett. Appl. Nanobiosci. 10 (2021) 2148–2166, https://doi.org/10.33263/LIANBS102.21482166.

[4] J.H. Deng, X.R. Zhang, G.M. Zeng, J.L. Gong, Q.Y. Niu, J. Liang, Simultaneous removal of Cd(II) and ionic dyes from aqueous solution using magnetic graphene oxide nanocomposite as an adsorbent, Chem. Eng. J. 226 (2013) 189–200, https://doi.org/10.1016/j.cej.2013.04.045.

[5] A. Markowicz, G. Płaza, Z. Piotrowska-Seget, Activity and functional diversity of microbial communities in long-term hydrocarbon and heavy metal contaminated soils, Arch. Environ. Prot. 42 (2016) 3–11, https://doi.org/10.1515/aep-2016-0041.

[6] P.T. Gauthier, W.P. Norwood, E.E. Prepas, G.G. Pyle, Metal-PAH mixtures in the aquatic environment: A review of co-toxic mechanisms leading to more-than-additive outcomes, Aquat. Toxicol. 154 (2014) 253–269, https://doi.org/10.1016/j.aquatox.2014.05.026.

[7] J. Bi, Q. Tao, X. Huang, J. Wang, T. Wang, H. Hao, Simultaneous decontamination of multi-pollutants: A promising approach for water remediation, Chemosphere 284 (2021), https://doi.org/10.1016/j.chemosphere.2021.131270.

[8] M.A. Polti, J.D. Aparicio, C.S. Benimeli, M.J. Amoroso, Simultaneous bioremediation of Cr(VI) and lindane in soil by actinobacteria, Int. Biodeterior. Biodegrad. 88 (2014) 48–55, https://doi.org/10.1016/j.ibiod.2013.12.004.

[9] G.J. Zhou, G.G. Ying, S. Liu, L.J. Zhou, Z.F. Chen, F.Q. Peng, Simultaneous removal of inorganic and organic compounds in wastewater by freshwater green microalgae, Environ. Sci. Process. Impacts. 16 (2014) 2018–2027, https://doi.org/10.1039/c4em00094c.

[10] M. Cao, Y. Hu, Q. Sun, L. Wang, J. Chen, X. Lu, Enhanced desorption of PCB and trace metal elements (Pb and Cu) from contaminated soils by saponin and EDDS mixed solution, Environ. Pollut. 174 (2013) 93–99, https://doi.org/10.1016/j.envpol.2012.11.015.

[11] Y. Li, B. Helmreich, Simultaneous removal of organic and inorganic pollutants from synthetic road runoff using a combination of activated carbon and activated lignite, Sep. Purif. Technol. 122 (2014) 6–11, https://doi.org/10.1016/j.seppur.2013.10.025.

[12] G. Yang, L. Tang, G. Zeng, Y. Cai, J. Tang, Y. Pang, Y. Zhou, Y. Liu, J. Wang, S. Zhang, W. Xiong, Simultaneous removal of lead and phenol contamination from water by nitrogen-functionalized magnetic ordered mesoporous carbon, Chem. Eng. J. 259 (2015) 854–864, https://doi.org/10.1016/j.cej.2014.08.081.

[13] X. Hu, H. Ji, F. Chang, Y. Luo, Simultaneous photocatalytic Cr(VI) reduction and 2,4,6-TCP oxidation over g-C3N4 under visible light irradiation, Catal. Today. 224 (2014) 34–40, https://doi.org/10.1016/j.cattod.2013.11.038.

[14] Y. Deng, L. Tang, G. Zeng, Z. Zhu, M. Yan, Y. Zhou, J. Wang, Y. Liu, J. Wang, Insight into highly efficient simultaneous photocatalytic removal of Cr(VI) and 2,4-diclorophenol under visible light irradiation by phosphorus doped porous ultrathin g-C3N4 nanosheets from aqueous media: Performance and reaction mechanism, Appl. Catal. B Environ. 203 (2017) 343–354, https://doi.org/10.1016/j.apcatb.2016.10.046.

[15] W. Chen, X. He, Z. Jiang, B. Li, X. Yan Li, L. Lin, A capacitive deionization and electro-oxidation hybrid system for simultaneous removal of heavy metals and organics from wastewater, Chem. Eng. J. 451 (2023) 139071, https://doi.org/10.1016/j.cej.2022.139071.

[16] V. Ya, N. Martin, Y.H. Chou, Y.M. Chen, K.H. Choo, S.S. Chen, C.W. Li, Electrochemical treatment for simultaneous removal of heavy metals and organics from surface finishing wastewater using sacrificial iron anode, J. Taiwan Inst. Chem. Eng. 83 (2018) 107–114, https://doi.org/10.1016/j.jtice.2017.12.004.

[17] L.P. Padhye, P. Srivastava, T. Jasemizad, S. Bolan, D. Hou, S.M. Shaheen, J. Rinklebe, D. O'Connor, D. Lamb, H. Wang, K.H.M. Siddique, N. Bolan, Contaminant containment for sustainable remediation of persistent contaminants in soil and groundwater, J. Hazard. Mater. 455 (2023), https://doi.org/10.1016/j.jhazmat.2023.131575.

[18] A. Kadier, Y. Simayi, P. Abdeshahian, N.F. Azman, K. Chandrasekhar, M.S. Kalil, A comprehensive review of microbial electrolysis cells (MEC) reactor designs and configurations for sustainable hydrogen gas production, Alexandria Eng. J. 55 (2016) 427–443, https://doi.org/10.1016/j.aej.2015.10.008.

[19] M. Tucci, A. Milani, M. Resitano, C.C. Viggi, O. Giampaoli, A. Miccheli, S. Crognale, B. Matturro, S. Rossetti, F. Harnisch, F. Aulenta, Syntrophy drives the microbial electrochemical oxidation of toluene in a continuous-flow "bioelectric well", J. Environ. Chem. Eng. 10 (2022) https://doi.org/10.1016/j.jece.2022.107799.

[20] C.C. Viggi, M. Tucci, M. Resitano, V. Palushi, S. Crognale, B. Matturro, M.P. Papini, S. Rossetti, F. Aulenta, Enhancing the Anaerobic Biodegradation of Petroleum Hydrocarbons in Soils with Electrically Conductive Materials, Bioengineering 10 (2023) 1–14.

[21] H. Friman, A. Schechter, Y. Nitzan, R. Cahan, Phenol degradation in bio-electrochemical cells, Int. Biodeterior. Biodegrad. 84 (2013) 155–160, https://doi.org/10.1016/j.ibiod.2012.04.019.

[22] U. Marzocchi, E. Palma, S. Rossetti, F. Aulenta, A. Scoma, Parallel artificial and biological electric circuits power petroleum decontamination: The case of snorkel and cable bacteria, Water Res. 173 (2020), https://doi.org/10.1016/j.watres.2020.115520.

[23] E. Palma, A. Espinoza Tofalos, M. Daghio, A. Franzetti, P. Tsiota, C. Cruz Viggi, M. P.M.P. Papini, F. Aulenta, Bioelectrochemical treatment of groundwater containing BTEX in a continuous-flow system: Substrate interactions, microbial community analysis, and impact of sulfate as a co-contaminant, N, Biotechnol. 53 (2019) 41–48, https://doi.org/10.1016/j.nbt.2019.06.004.

[24] T. Zhang, S.M. Gannon, K.P. Nevin, A.E. Franks, D.R. Lovley, Stimulating the anaerobic degradation of aromatic hydrocarbons in contaminated sediments by providing an electrode as the electron acceptor, Environ. Microbiol. (2010), https://doi.org/10.1111/j.1462-2920.2009.02145.x.

[25] M. Tucci, C.C. Viggi, M. Resitano, B. Matturro, S. Crognale, I. Pietrini, S. Rossetti, F. Harnisch, F. Aulenta, Simultaneous removal of hydrocarbons and sulfate from groundwater using a "bioelectric well", Electrochim. Acta. 388 (2021) 138636 https://doi.org/10.1016/j.electacta.2021.138636.

[26] M. Tucci, C. De Laurentiis, M. Resitano, C.C. Viggi, Membrane-Less Bioelectrochemical Reactor for the Treatment of Groundwater Contaminated by Toluene and Trichloroethene, Chem. Eng. Trans. 93 (2022) 85–90, https://doi.org/10.3303/CET2293015.

[27] O. Modin, X. Wang, X. Wu, S. Rauch, K.K. Fedje, Bioelectrochemical recovery of Cu, Pb, Cd, and Zn from dilute solutions, J. Hazard. Mater. 235–236 (2012) 291–297, https://doi.org/10.1016/j.jhazmat.2012.07.058.

[28] S. Wang, A. Adekunle, V. Raghavan, Bioelectrochemical systems-based metal removal and recovery from wastewater and polluted soil: Key factors, development, and perspective, J. Environ. Manage. 317 (2022) 115333, https://doi.org/10.1016/j.jenvman.2022.115333.

[29] H. Wang, Z.J. Ren, Bioelectrochemical metal recovery from wastewater: A review, Water Res. 66 (2014) 219–232, https://doi.org/10.1016/j.watres.2014.08.013.

[30] B. Hemdan, V.K. Garlapati, S. Sharma, S. Bhadra, S. Maddirala, K.M. Varsha, V. Motru, P. Goswami, S. Sevda, T.M. Aminabhavi, Bioelectrochemical systems-based metal recovery: Resource, conservation and recycling of metallic industrial effluents, Environ. Res. 204 (2022) 112346, https://doi.org/10.1016/j.envres.2021.112346.

[31] M.Y. Mitov, I.O. Bardarov, E.Y. Chorbadzhiyska, Y.V. Hubenova, Copper recovery combined with wastewater treatment in a microbial fuel cell, Bulg. Chem. Commun. 50 (2018) 136–140.

[32] X. Zhang, D. Zhang, Y. Huang, K. Zhang, P. Lu, Simultaneous removal of organic matter and iron from hydraulic fracturing flowback water through sulfur cycling in a microbial fuel cell, Water Res. 147 (2018) 461–471, https://doi.org/10.1016/j.watres.2018.10.020.

[33] E. Gambino, K. Chandrasekhar, R.A. Nastro, SMFC as a tool for the removal of hydrocarbons and metals in the marine environment: a concise research update, Environ. Sci. Pollut. Res. 28 (2021), https://doi.org/10.1007/s11356-021-13593-3.

[34] C. Cruz Viggi, M. Tucci, M. Resitano, S. Crognale, M.L. Di Franca, S. Rossetti, F. Aulenta, Coupling of bioelectrochemical toluene oxidation and trichloroethene reductive dechlorination for single-stage treatment of groundwater containing multiple contaminants, Environ. Sci. Ecotechnology. 11 (2022), https://doi.org/10.1016/j.ese.2022.100171.

[35] M. Tucci, D. Fernández-Verdejo, M. Resitano, P. Ciacia, A. Guisasola, P. Blánquez, E. Marco-Urrea, C. Cruz Viggi, B. Matturro, S. Crognale, F. Aulenta, Toluene-driven anaerobic biodegradation of chloroform in a continuous-flow bioelectrochemical reactor, Chemosphere 338 (2023), https://doi.org/10.1016/j.chemosphere.2023.139467.

[36] V. Zanello, L.E. Scherger, C. Lexow, Assessment of groundwater contamination risk by BTEX from residual fuel soil phase, SN Appl. Sci. 3 (2021), https://doi.org/10.1007/s42452-021-04325-w.
[37] C.C. Viggi, S. Colantoni, F. Falzetti, A. Bacaloni, D. Montecchio, F. Aulenta, Conductive Magnetite Nanoparticles Enhance the Microbial Electrosynthesis of Acetate from CO2 while Diverting Electrons away from Methanogenesis, Fuel Cells 20 (2020), https://doi.org/10.1002/fuce.201900152.
[38] R. Sander, Compilation of Henry's law constants (version 4.0) for water as solvent, Atmos. Chem. Phys. 15 (2015) 4399–4981, https://doi.org/10.5194/acp-15-4399-2015.
[39] M.L. Di Franca, B. Matturro, S. Crognale, M. Zeppilli, E. Dell'Armi, M. Majone, M. Petrangeli Papini, S. Rossetti, Microbiome Composition and Dynamics of a Reductive/Oxidative Bioelectrochemical System for Perchloroethylene Removal: Effect of the Feeding Composition, Front. Microbiol. 13 (2022), https://doi.org/10.3389/fmicb.2022.951911.
[40] B. Matturro, M. Zeppilli, A. Lai, M. Majone, S. Rossetti, Metagenomic Analysis Reveals Microbial Interactions at the Biocathode of a Bioelectrochemical System Capable of Simultaneous Trichloroethylene and Cr(VI) Reduction, Front. Microbiol. 12 (2021), https://doi.org/10.3389/fmicb.2021.747670.
[41] B.J. Callahan, P.J. McMurdie, M.J. Rosen, A.W. Han, A.J.A. Johnson, S.P. Holmes, DADA2: High-resolution sample inference from Illumina amplicon data, Nat. Methods. 13 (2016), https://doi.org/10.1038/nmeth.3869.
[42] S. Mathews, M. Hans, F. Mücklich, M. Solioz, Contact killing of bacteria on copper is suppressed if bacterial-metal contact is prevented and is induced on iron by copper ions, Appl. Environ. Microbiol. 79 (2013), https://doi.org/10.1128/AEM.03608-12.
[43] B. Korth, A. Kuchenbuch, F. Harnisch, Availability of Hydrogen Shapes the Microbial Abundance in Biofilm Anodes based on Geobacter Enrichment, ChemElectroChem 7 (2020), https://doi.org/10.1002/celc.202000731.
[44] L.P. Singha, P. Pandey, Rhizobacterial community of Jatropha curcas associated with pyrene biodegradation by consortium of PAH-degrading bacteria, Appl. Soil Ecol. 155 (2020), https://doi.org/10.1016/j.apsoil.2020.103685.
[45] X. Zhang, B. Li, H. Wang, X. Sui, X. Ma, Q. Hong, R. Jiang, Rhizobium petrolearium sp. nov., isolated from oilcontaminated soil, Int. J. Syst. Evol. Microbiol. 62 (2012), https://doi.org/10.1099/ijs.0.026880-0.
[46] Y. Teng, X. Wang, L. Li, Z. Li, Y. Luo, Rhizobia and their bio-partners as novel drivers for functional remediation in contaminated soils, Front. Plant Sci. 6 (2015), https://doi.org/10.3389/fpls.2015.00032.
[47] A. Konya, B.A. Fiddler, O. Bunch, K.Z. Hess, C. Ferguson, M.J. Krzmarzick, Lead or cadmium co-contamination alters benzene and toluene degrading bacterial communities, Biodegradation 34 (2023) 357–369, https://doi.org/10.1007/s10532-023-10021-w.
[48] N.T. Phung, J. Lee, K.H. Kang, I.S. Chang, G.M. Gadd, B.H. Kim, Analysis of microbial diversity in oligotrophic microbial fuel cells using 16S rDNA sequences, FEMS Microbiol. Lett. 233 (2004) 77–82, https://doi.org/10.1016/j.femsle.2004.01.041.
[49] P. Chen, L. Zhang, X. Guo, X. Dai, L. Liu, L. Xi, J. Wang, L. Song, Y. Wang, Y. Zhu, L. Huang, Y. Huang, Diversity, biogeography, and biodegradation potential of actinobacteria in the deep-sea sediments along the southwest Indian ridge, Front. Microbiol. 7 (2016), https://doi.org/10.3389/fmicb.2016.01340.
[50] R. Laso-Pérez, C. Hahn, D.M. Van Vliet, H.E. Tegetmeyer, F. Schubotz, N.T. Smit, T. Pape, H. Sahling, G. Bohrmann, A. Boetius, K. Knittel, G. Wegenera, Anaerobic degradation of non-methane alkanes by "candidatus methanoliparia" in hydrocarbon seeps of the gulf of Mexico, MBio 10 (2019), https://doi.org/10.1128/mBio.01814-19.
[51] M.A. Khomyakova, D.G. Zavarzina, A.Y. Merkel, A.A. Klyukina, V.A. Pikhtereva, S. N. Gavrilov, A.I. Slobodkin, The first cultivated representatives of the actinobacterial lineage OPB41 isolated from subsurface environments constitute a novel order Anaerosomatales, Front. Microbiol. 13 (2022) 1–16, https://doi.org/10.3389/fmicb.2022.1047580.
[52] L. Szydlowski, J. Ehlich, P. Szczerbiak, N. Shibata, I. Goryanin, Novel species identification and deep functional annotation of electrogenic biofilms, selectively enriched in a microbial fuel cell array, Front. Microbiol. 13 (2022), https://doi.org/10.3389/fmicb.2022.951044.
[53] Y. Kang, H. Ma, Z. Jing, C. Zhu, Y. Li, H. Wu, P. Dai, Z. Guo, J. Zhang, Enhanced benzofluoranthrene removal in constructed wetlands with iron- modified biochar: Mediated by dissolved organic matter and microbial response, J. Hazard. Mater. 443 (2023), https://doi.org/10.1016/j.jhazmat.2022.130322.
[54] X. Li, Y. Li, X. Zhang, X. Zhao, Y. Sun, L. Weng, Y. Li, Long-term effect of biochar amendment on the biodegradation of petroleum hydrocarbons in soil microbial fuel cells, Sci. Total Environ. 651 (2019) 796–806, https://doi.org/10.1016/j.scitotenv.2018.09.098.
[55] A. Ferraro, G. Massini, V.M. Miritana, A. Panico, L. Pontoni, M. Race, S. Rosa, A. Signorini, M. Fabbricino, F. Pirozzi, Bioaugmentation strategy to enhance polycyclic aromatic hydrocarbons anaerobic biodegradation in contaminated soils, Chemosphere 275 (2021), https://doi.org/10.1016/j.chemosphere.2021.130091.
[56] L.H. Yang, H.Y. Cheng, T.T. Zhu, H.C. Wang, M.R. Haider, A.J. Wang, Resorcinol as a highly efficient aromatic electron donor in bioelectrochemical system, J. Hazard. Mater. 408 (2021), https://doi.org/10.1016/j.jhazmat.2020.124416.
[57] C.W. Lin, T.J. Zhu, L.C. Lin, S.H. Liu, Promoting biodegradation of toluene and benzene in groundwater using microbial fuel cells with cathodic modification, J. Water Process Eng. 47 (2022), https://doi.org/10.1016/j.jwpe.2022.102839.
[58] B. Hashemi, S.J. Horn, J.J. Lamb, K.M. Lien, Potential role of sulfide precipitates in direct interspecies electron transfer facilitation during anaerobic digestion of fish silage, Bioresour. Technol. Reports. 20 (2022), https://doi.org/10.1016/j.biteb.2022.101264.
[59] Y. Sui, W. Fu, H. Yang, Y. Zeng, Y. Zhang, Q. Zhao, Y. Li, X. Zhou, Y. Leng, M. Li, G. Zou, Low temperature synthesis of Cu2O crystals: Shape evolution and growth mechanism, Cryst. Growth Des. 10 (2010) 99–108, https://doi.org/10.1021/cg900437x.
[60] J. Xu, K. Yu, Z. Zhu, Synthesis and field emission properties of Cu dendritic nanostructures, Phys. E Low-Dimensional Syst. Nanostruct. 42 (2010) 1451–1455, https://doi.org/10.1016/j.physe.2009.11.115.
[61] M.V. Mandke, H.M. Pathan, Electrochemical growth of copper nanoparticles: Structural and optical properties, J. Electroanal. Chem. 686 (2012), https://doi.org/10.1016/j.jelechem.2012.09.004.
[62] D.B. Pedersen, S. Wang, S.H. Liang, Charge-transfer-driven diffusion processes in Cu@Cu-oxide core-shell nanoparticles: Oxidation of 3.0 ± 0.3 nm diameter copper nanoparticles, J. Phys. Chem. c. 112 (2008), https://doi.org/10.1021/jp710619r.
[63] O.A. Yeshchenko, I.M. Dmitruk, A.M. Dmytruk, A.A. Alexeenko, Influence of annealing conditions on size and optical properties of copper nanoparticles embedded in silica matrix, Mater. Sci. Eng. b. 137 (2007), https://doi.org/10.1016/j.mseb.2006.11.030.
[64] F. Pagnanelli, Shape evolution and effect of organic additives in the electrosynthesis of Cu nanostructures, J. Solid State Electrochem. 23 (2019), https://doi.org/10.1007/s10008-019-04360-z.